Curvature measurements to improve polymer integration in microelectronic devices

Benjamin Vavrille, Lionel Vignoud, Laurent-Luc Chapelon, Rafael Estevez

Curvature measurements to improve polymer integration in microelectronic devices

Benjamin Vavrille
Plasma
STMicroelectronics
Crolles, France
benjamin.vavrille@st.com

Lionel Vignoud
DPFT
Univ. Grenoble Alpes, CEA, Leti
Grenoble, France
lionel.vignoud@cea.fr

Laurent-Luc Chapelon
Plasma
STMicroelectronics
Crolles, France
laurent-luc.chapelon@st.com

Rafael Estevez
Materials Science Departement
Univ. Grenoble Alpes, CNRS, SIMaP
Grenoble, France
rafael.estevez@simap.grenoble-inp.fr

***Abstract*—Thermoset resins are singular in the aim of microelectronics. Exhibiting a high contrast of thermomechanical properties with other materials like oxides or metals, polymers can threaten the mechanical integrity of stacks. Knowing polymer properties allows manufacturers to foresee the compatibility of materials and improve chipsets reliability. The thermally induced curvature approach uses this incompatibility to determine the biaxial modulus and the coefficient of thermal expansion of a film on a substrate. This method can not only check the achievement of the polymers cross-linking, but also estimate their glass transition temperature. In this paper, we show the ability of this technique to, not only, measure those properties at glassy state, but also, for the first time, at rubbery state.**

Keywords—Thermally induced curvature, polymer, coefficient of thermal expansion, Young's modulus, Poisson's ratio, glass transition, thermal stress, bilayer, characterization techniques, glassy state, rubbery state, ellipsometry, picosecond ultrasonics

I. Introduction

Thermosets are very common in microelectronics for pattern transfer and insulation, but can easily be a threat for stacks and related mechanical integrity. Polymers exhibit larger coefficients of thermal expansion (CTE) and lower elastic moduli (M) than metals, oxides or silicon. The mismatch of the thermomechanical properties can cause significant strain contrast and induce failure or cracking. Upon heating, the thermal expansion of a thermoset can harm its encapsulating layer of low CTE due to this contrast. The tensile stress in the encapsulation increases until cracks appear, allowing the penetration of humidity and reducing chipsets reliability. This can be prevented from an analysis of the induced stress distribution at each deposition stage with calculations considering a multi-layers structure [1]. This requires knowledge of materials thermomechanical properties and, in this case, those of the polymer layer. The amorphous polymer under consideration can be in both the glassy and rubbery states during multiple temperature cycles. This leads to drastic changes in film properties, such as Young's modulus dropping from 1-5 GPa to hundreds of MPa and CTE becoming relatively large. Consequently, to improve the integration of a thermoset layer, its glass transition temperature T_g, its elastic modulus and its CTE have to be identified.

Due to materials structure and deposition process, films properties can differ from those of bulk materials [2]–[4]. Dedicated methods to study film on substrate must be developed like ellipsometry and nano-indentation. Furthermore, some polymers can exhibit anisotropy leading to dissimilarity between in-plane and out-of-plane mechanical properties. This heterogeneity can be explained by the in-plane molecular orientation of the polymeric chains induced by the spin-coating deposition process [5], [6]. For these reasons, elaborating in-plane characterization techniques is necessary to study the evolution of materials properties with temperature at the microscale. In this paper, we present a thermally induced curvature approach to characterize film properties. This non-destructive technique has the great advantage to estimate simultaneously the CTE, the Young's modulus and the glass transition temperature. Properties are obtained by comparing the thermally induced curvature of (at least) two different substrates where the same thin film material is deposited. Metals [7], [8], oxide [9] and polymers [10] thin layers properties have previously been predicted with this approach, but only at glassy state for thermosets. We introduce our methodology of the double-substrate technique and its application to a thermoset. The thermomechanical properties of the retained material can be estimated not only at glassy but also at rubbery state. Results are compared with colored picosecond acoustics (APiC), an ultrafast acoustic technique, and ellipsometry measurements on the same material.

II. Theory

We consider an elastic bilayer made of a film deposited on a substrate. Layer thicknesses are noted h_i with i=s or f, for substrate and film, respectively. Their biaxial modulus M_i and CTE α_i are distinct which leads to a temperature-dependent misfit stress in the film [1]

$$\sigma_f(T) = M_f(\alpha_s - \alpha_f)\,\Delta T \qquad (1)$$

for a given temperature variation ΔT. Intrinsic stresses are not taken into account in this model, so inelastic strain is thermal that induces a stress in both parts due to the CTE mismatch between the film and substrate. Indeed, polymers do not seem to generate any intrinsic stress during spin-coating or curing on wafers [5].

The mismatch of properties generates a deformation of the bilayer with the overall wafer becoming spherically bent for isotropic constitutive layers and homogeneous thicknesses. The induced wafer curvature is denoted $\kappa(T)$ and $\Delta\kappa = \kappa - \kappa_0$, κ_0 being the initial curvature of the substrate. By introducing the thicknesses and modulus ratio, respectively h and m, as

$h=h_f / h_s$ and $m = M_f / M_s$, the curvature variation can be expressed as

$$\Delta\kappa = \frac{1+h}{1+2hm(2+3h+2h^2)+h^4m^2} \frac{6hm}{h_s} (\alpha_s - \alpha_f) \Delta T \qquad (2)$$

with $\Delta T = T - T_0$, T_0 being a reference temperature [1]. This model is a generalization of Stoney's one. It has the benefit of being effective for any h and m ratios for an uniform mismatch stress in the film [11]. Therefore, curvature κ is the sign of the incompatibility between film and substrate properties. The CTE difference is often substantial with polymer because they exhibit larger CTE than common substrate materials.

With temperature-independent modulus M_i and CTE α_i, the curvature evolution is linear with T, according to (2) and film properties can be derived by depositing the same thin polymer film on two different substrates [12]. Moreover, polymer properties can be thickness-dependent [2]–[4], that is why formula (2) is preferred with polymeric films instead of the well-known Stoney expression [13].

Furthermore, a sensitivity analysis has shown that the uncertainties of guessed properties M_f and α_f are proportional to the factor

$$C_i = \frac{|\alpha_f - \alpha_{s,1}|}{|\alpha_{s,2} - \alpha_{s,1}|} \qquad (3)$$

with $\alpha_{s,i}$ the CTE of substrate i ($i=1$ or 2). These uncertainties are directly related to the induced curvature and the choice of substrates but not to the experimental procedure. Equation (3) shows the importance to take substrates with distinct CTE to maximize the difference $|\alpha_{s,2} - \alpha_{s,1}|$, in order to minimize those uncertainties. Because of the inherent contrast of CTE between polymer and substrate materials, uncertainties are larger to those with oxides or metals.

III. Materials and Experimental Technique

A thermoset polymer has been deposited by spin coating on silicon (Si) and gallium arsenide (GaAs) substrates. Polymerization is achieved by a specific annealing at high temperature. Substrate materials have been chosen because they show a distinct CTE: 3.3 ppm/K and 6.2 ppm/K for Si and GaAs, respectively. To increase the measuring range and thus optimize the sensitivity of the measuring tool, substrates are thinned down to 300 microns by grinding and then polishing.

Curvature measurements have been performed with the kSA MOS Thermal Scan tool by using a multi-beam optical stress sensor, in an oven with a nitrogen flux at low pressure

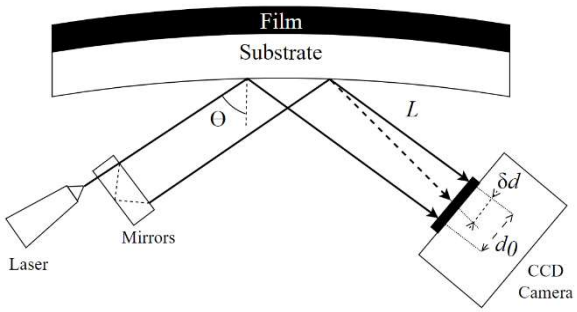

Fig. 1 Curvature measurement set-up of a multi-beam optical stress sensor.

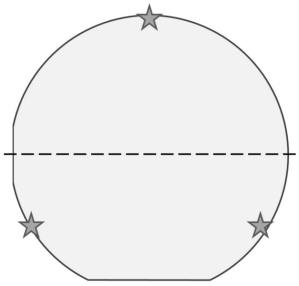

Fig. 2 Wafer positioning in kSA MOS Thermal Scan. Dashed line show the scanning path and stars symbolize the support points.

(100mbar). Local curvature κ is obtained from the relative spacing ($\delta d/d_0$) of six light spots from the expression

$$\kappa = \frac{\delta d}{d_0} \frac{\cos(\Theta)}{2L} \qquad (4)$$

with d_0 the initial spacing between beams, δd the beam spacing difference from d_0. Fig. 1. shows the angle of incidence of the beams Θ and the distance L between the camera and the plate normal. Equation (4) is commonly combined with the well-known Stoney formula to express the stress-temperature relationship. In this case, properties identification is performed with the film stress $\sigma_f(T)$ as a raw data, as in [10], but Stoney's assumption are not met here. Therefore, using the curvature variation with temperature and a full bilayer description is necessary.

Wafers are set on three points equally spaced (see Fig. 2). Due to the effect of gravity-induced deflection and the presence of pins, substrates display an initial curvature κ_0. Therefore, curvature measurements with temperature are done before and after deposition. In order to reduce the uncertainties and experimental time, curvature is averaged over a diameter line, dashed in Fig. 2.

Conversely to κ_0, the measurement of $\kappa(T)$ is performed during three thermal cycles. Due to humidity and solvent desorption, the first cycle is usually different from the following cycles [14]. The other cycles are reproducible, meaning that the polymer is stable and fully cured. Thicknesses and substrates properties in (2) are measured or borrowed from the literature. Film thicknesses uniformity is verified by ellipsometry.

To verify curvature results, APiC and temperature-dependent ellipsometry measurements have been carried out to estimate the biaxial modulus and CTE, respectively. APiC measurements have been carried out on an experimental set-up at IEMN laboratory of Lille, France. The difference between colored picosecond acoustics with other ultrafast acoustic techniques is the use of different wavelengths for the pump and the probe. The former is near infrared and the latter is close to blue. Indeed, the material's response can be enhanced using lower wavelengths [15]. Because the resin is transparent and non-absorbent, a thin metal layer is added between the polymer and silicon as a transducer. This way, the metal will generate the pulse strain to be detected by the probe. The longitudinal sound's velocity V_L is usually obtained from the oscillation period. In acoustic, the square of the measured velocity V_L multiplied by the film's density ρ is a reduced modulus $M_r = V_L^2 \rho$. The mass density ρ is obtain by combining a mass measurement with a micrometric scale and a thickness measurement.

APiC and curvature-based approach measure different reduced moduli M_r. The curvature technique measures the biaxial modulus of the film M_f and with acoustic, the square of the velocity V_L is multiplied by density. Thus, we chose to compare Young's modulus E by assuming a range of possible values for the Poisson's ratio ν. The relationships between Young's moduli E and reduced moduli M_r are recapped in Table I.

TABLE I. RELATIONSHIP BETWEEN YOUNG'S MODULI E AND REDUCED MODULI M_r

Methods	References	Young's Modulus E
Curvature	[12]	$(1-\nu)\,M_r$
APiC	[16], [17]	$\frac{(1-2\nu)(1+\nu)}{(1-\nu)}M_r$

Also, CTE from ellipsometry measurements is estimated from the thickness variation with temperature $h_f(T)$ as:

$$\alpha_f = \frac{(1-\nu)}{(1+\nu)}\frac{h_f - h_{f0}}{h_{f0}\Delta T} + \frac{2\nu}{(1+\nu)}\alpha_s \qquad (5)$$

where h_{f0} and h_f are respectively the initial and final film thickness, for a given temperature interval ΔT [18]. Ellipsometry measurements are also performed with a Woolam *RC2*. Samples thicknesses are measured during two thermal cycles, again to get rid of possible presence of humidity during the first one.

For a glassy thermoset, the Poisson ratio ranges from 0.35 to 0.43. To enhance the cross-comparison, we choose to calculate Young's modulus with a Poisson ratio at 0.35, 0.40 and 0.43. At the rubbery state, incompressibility suggests a Poisson ratio close to 0.49. The CTE from ellipsometry also requires the knowledge of this parameter whereas the one estimated by curvature measurements is the only property obtained directly.

IV. Results and Discussion

The curvature variation with temperature is bilinear, as reported in Fig. 3, with a singular and systematic change of slope at 358 K for both wafers. The slope drops by 80% for both substrates. The complete polymer reticulation is confirmed by the repeatability of this particular behavior. The discontinuity is likely the sign of glass transition. After such transition, the slope of the curvature is usually close to zero as Young modulus drops by three decades and stress in the film became negligible in the rubbery state [10]. Because it is not the case in our experiment, the rubbery state can be characterized using the observed linear curvature variation with temperature. The methodology remains the same for both states. Averaged polymer properties will be derived for the glassy state between 293 and 358 K and between 358 and 473K for the rubbery polymer. According to (2), the linear variations of curvature indicate that elastic modulus and CTE are temperature-independent. In order to reduce uncertainties, we measure with high precision: wafer thicknesses with confocal microscopy, films thickness and uniformity with ellipsometry. Values are given in Table II. Film thicknesses are uniform according to ellipsometry with a coefficient of variation over 98%. Substrates properties (M_s and α_s in (2)) in Table II are averaged on each interval and are estimated with [19], [20] for silicon and with [21], [22], for GaAs.

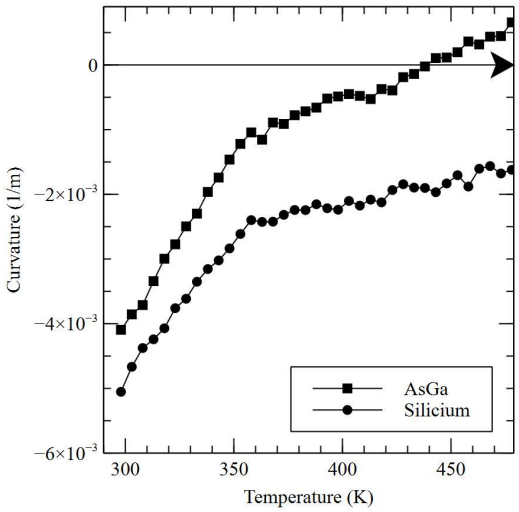

Fig. 3 Post-processed curvature Δκ measured for the polymer film on silicon and AsGa wafers, after humidity evacuation

TABLE II. PROPERTIES OF FILMS AND SUBSTRATES

Substrate	Silicon	Gallium Arsenide
h_s (μm)	298	293
h_f (nm)	446	441
M_s (GPa) (293 - 358 K)	178	121
α_s (ppm/K) (293 - 358 K)	2.8	5.8
M_s (GPa) (358 - 473 K)	179	121
α_s (ppm/K) (358 - 473 K)	3.3	6.2

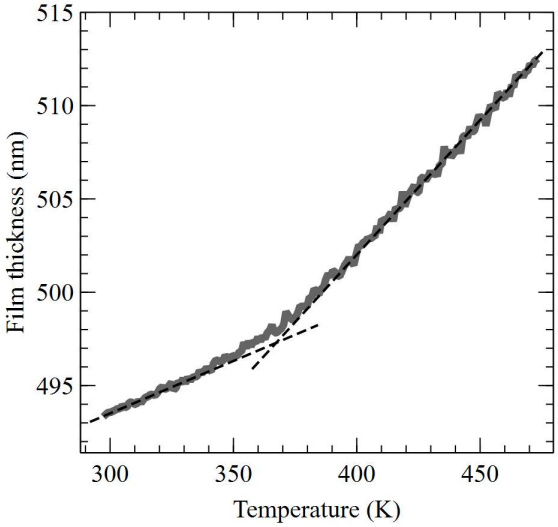

Fig. 4 Film thickness evolution monitored by ellipsometry after humidity evacuation for the polymer film on a silicon substrate

Temperature-dependent ellipsometry estimates the thickness evolution upon heating and cooling. Similarly to the curvature method, T_g can be determined from the analysis of raw ellipsometric data [23]. Fig. 4 shows the film thickness $h_f(T)$ evolution with temperature from 293 to 473 K. The thickness $h_f(T)$ is also bilinear with a systematic break around 358 K during the thermal transition of the polymer, corroborating the curvature estimation of T_g. Hence, there is no major temperature shift between these experiments.

Using ultrafast acoustic on polymer is not a standard technique. However, this appears sensitive enough to capture the glass transition [24], [25]. The measured sound velocity, shown in Fig. 5, exhibits a drop of slope by 10% between 350 and 370K, which corresponds to the polymer relaxation.

The results for Young's moduli characterizations are recapped in Fig. 6 and Table III. According to the curvature approach, at glassy state, the modulus is around 5 GPa which is realistic for a thermoset. Beyond T_g, the modulus drops to a few hundred MPa, as expected.

TABLE III. YOUNG'S MODULI OBTAINED FROM CURVATURE-BASED TECHNIQUE AND APIC MEASUREMENTS.

Poisson's ratio	State	Young's Modulus *E* (GPa)	
		Curvature	APiC
0.35	Glass	5.3 ± 1.3	5.6 ± 1.4
0.40		4.9 ± 1.2	4.2 ± 1.1
0.43		4.7 ± 1.1	3.2 ± 0.8
0.49	Rubber	0.24 ± 0.20	0.39 ± 0.10

Due to the set-up limitation, APiC measurements are discontinuous and limited to 423K. Therefore, results are average between 293 and 358K for the glassy thermoset and between 373 and 423K at rubbery state. We obtain a good agreement between APiC and curvature-based approach for both state. As illustrated in Fig. 6, the possible range for the Young modulus E is smaller for curvature than APiC, mainly due to the high dependence on the assumption for the Poisson ratio, looking at the expressions in Table I.

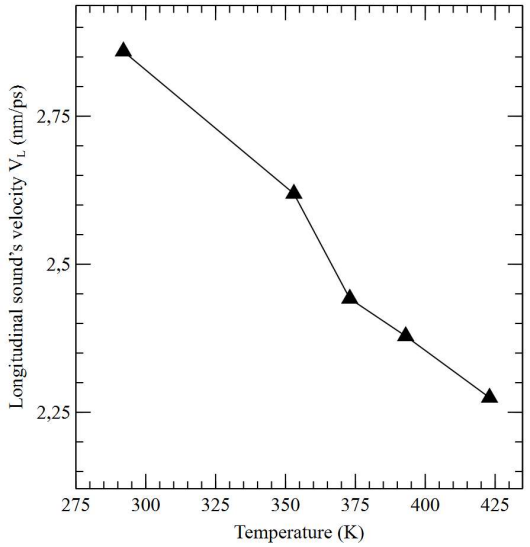

Fig. 5. Longitudinal sound's velocity and density measured with APiC

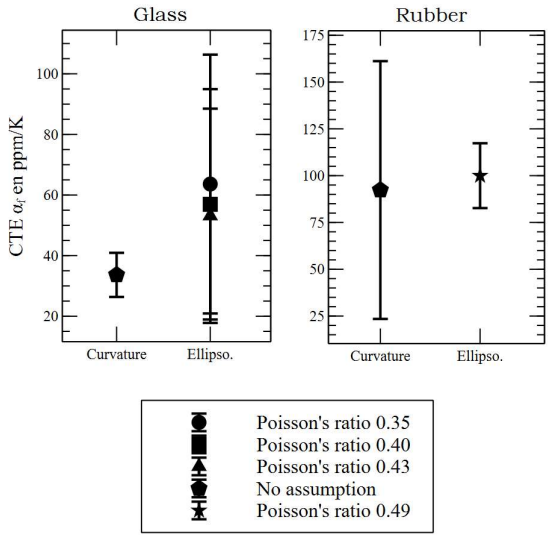

Fig. 6. CTE obtained from curvature-based approach and temperature-dependent ellipsometry.

The CTE derived by curvature measurement and ellipsometry are shown in Fig. 7 and Table IV. CTE are estimated on the same temperature intervals 293–358K and 358–473K. Regarding the curvature approach, the CTE increases from 34 ppm/K to 92 ppm/K with the glass transition. Conversely to the modulus, the CTE increases after the relaxation, as expected. In return, the coefficient C_i, from (3), is about 10 at glass and around 31 beyond T_g, leading to relative uncertainties of properties almost 3 times larger after T_g. This is mainly due to the choice of substrates: the CTE of the substrates are smaller than the polymer's one.

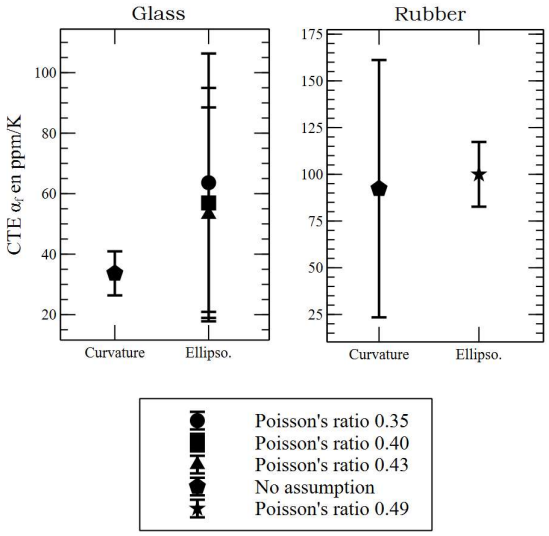

Fig. 7. CTE obtained from curvature-based approach and temperature-dependent ellipsometry.

Nevertheless, the errors for Young's moduli are admissible in Fig. 6.

For temperature-dependent ellipsometry, at glassy state, the uncertainties are relatively large (over 30 ppm/K) owing to (i) the small expansion of the film (+3nm) and (ii) the uncertainty of the film thickness h_f estimated to be ±2nm. Beyond T_g, for the same reasons, the CTE uncertainty is reduced because the film expands around 16 ± 2nm.

Thus, in Fig. 7, we can see the cross-comparison of CTE between curvature approach and ellipsometry. Corroboration is moderate before the glass transition and correct at rubbery state. Above T_g, a discrepancy has been observed on polyimide. Thin film anisotropy can be explained by the in-plane orientation of the polymer chain caused by the spin-coating deposition process [5], [6]. Ultimately, APiC and ellipsometry measure out-of-plane properties, whereas curvature approach determines in-plane properties but anisotropy is not always verified. In our case, such anisotropy seems unlikely because Young's modulus and CTE are quite comparable between techniques, meaning that the film remains isotropic.

TABLE IV. CTE OBTAINED FROM CURVATURE-BASED APPROACH AND TEMPERATURE-DEPENDENT ELLIPSOMETRY.

Poisson's ratio	**State**	**CTE (ppm/K)**	
		Curvature	**Ellipsometry**
No assumption	Glass	34 ± 7	
0.35			64 ± 43
0.40			57 ± 38
0.43			53 ± 35
No assumption	Rubber	92 ± 69	
0.49			100 ± 17

V. CONCLUSION

The thermally induced curvature technique has the benefit of being nondestructive, easy to carry out and provide average estimations of the thermomechanical properties on the entire surface rather than local ones. It allows the estimation of the glass transition of the thermoset and the measurement of the thermomechanical properties at glassy and rubbery states, if the slope of curvature are non-zero. Furthermore, the retained model in part II has to be preferred to Stoney's as the thickness ratio between film and substrate does not always meet Stoney assumptions for the measures of the curvature with temperature. Hence, the curvature-temperature relationship is available for any bilayer with an arbitrary thickness and modulus ratio. Young's modulus can be derived from curvature by assuming a range for the Poisson ratio. Fortunately, for thermosets, the range of this latter is known and then can be reduced by making a cross-comparison with other techniques (APiC, nano-indentation…)

For the polymer film under consideration, Young modulus from APiC corroborates well the results from the curvature-based characterization. Besides, CTE estimations from ellipsometry and curvature approach agree. Both estimation of temperature T_g are similar. Finally, these results can supply mechanical simulations to prevent stacks from cracks.

ACKNOWLEDGMENT

Part of this work, carried out on the Platform for Nanocharacterisation (PFNC), was supported by the "Recherche Technologique de Base" program of the French National Research Agency (ANR).

Special thanks to IEMN lab, Fabien Chevreux and Christophe Licitra for their measurements.

REFERENCES

[1] A. G. Evans and J. W. Hutchinson, "The thermomechanical integrity of thin films and multilayers," Acta Metall. Mater., vol. 43, no. 7, pp. 2507–2530, Jul. 1995, doi: 10.1016/0956-7151(94)00444-M.

[2] M. Liu, J. Sun, Y. Sun, C. Bock, and Q. Chen, "Thickness-dependent mechanical properties of polydimethylsiloxane membranes," J. Micromechanics Microengineering, vol. 19, no. 3, p. 035028, Mar. 2009, doi: 10.1088/0960-1317/19/3/035028.

[3] L. Li, N. Alsharif, and K. A. Brown, "Confinement-Induced Stiffening of Elastomer Thin Films," J. Phys. Chem. B, vol. 122, no. 47, pp. 10767–10773, Nov. 2018, doi: 10.1021/acs.jpcb.8b08779.

[4] L. Singh, P. J. Ludovice, and C. L. Henderson, "Influence of molecular weight and film thickness on the glass transition temperature and coefficient of thermal expansion of supported ultrathin polymer films," Thin Solid Films, vol. 449, no. 1–2, pp. 231–241, Feb. 2004, doi: 10.1016/S0040-6090(03)01353-1.

[5] G. Elsner, J. Kempf, J. W. Bartha, and H. H. Wagner, "Anisotropy of thermal expansion of thin polyimide films," Thin Solid Films, vol. 185, no. 1, pp. 189–197, Feb. 1990, doi: 10.1016/0040-6090(90)90018-9.

[6] H. C. Liou, P. S. Ho, and R. Stierman, "Thickness dependence of the anisotropy in thermal expansion of PMDA-ODA and BPDA-PDA thin films," Thin Solid Films, vol. 339, no. 1–2, pp. 68–73, 1999, doi: 10.1016/S0040-6090(98)01065-7.

[7] J. Jou and L. Hsu, "Stress analysis of elastically anisotropic bilayer structures," J. Appl. Phys., vol. 69, no. 3, pp. 1384–1388, Feb. 1991, doi: 10.1063/1.347277.

[8] Y. Y. Hu and W. M. Huang, Handbook of Manufacturing Engineering and Technology. London: Springer London, 2013.

[9] J. Zhao, T. Ryan, P. S. Ho, A. J. McKerrow, and W. Shih, "Measurement of elastic modulus, Poisson ratio, and coefficient of thermal expansion of on-wafer submicron films," J. Appl. Phys., vol. 85, no. 9, pp. 6421–6424, May 1999, doi: 10.1063/1.370146.

[10] J.-H. Zhao, M. Kiene, C. Hu, and P. S. Ho, "Thermal stress and glass transition of ultrathin polystyrene films," Appl. Phys. Lett., vol. 77, no. 18, pp. 2843–2845, Oct. 2000, doi: 10.1063/1.1322049.

[11] L. B. Freund, J. A. Floro, and E. Chason, "Extensions of the Stoney formula for substrate curvature to configurations with thin substrates or large deformations," Appl. Phys. Lett., vol. 74, no. 14, pp. 1987–1989, Apr. 1999, doi: 10.1063/1.123722.

[12] T. F. Retajczyk and A. K. Sinha, "Elastic stiffness and thermal expansion coefficients of various refractory silicides and silicon nitride films," Thin Solid Films, vol. 70, no. 2, pp. 241–247, 1980, doi: 10.1016/0040-6090(80)90364-8.

[13] G. G. Stoney, "The tension of metallic films deposited by electrolysis," Proc. R. Soc. London. Ser. A, Contain. Pap. a Math. Phys. Character, vol. 82, no. 553, pp. 172–175, May 1909, doi: 10.1098/rspa.1909.0021.

[14] J. Thurn and T. Hermel-Davidock, "Thermal stress hysteresis and stress relaxation in an epoxy film," J. Mater. Sci., vol. 42, no. 14, pp. 5686–5691, Jul. 2007, doi: 10.1007/s10853-006-0654-y.

[15] A. Devos, "Colored ultrafast acoustics: From fundamentals to applications," Ultrasonics, vol. 56, pp. 90–97, Feb. 2015, doi: 10.1016/j.ultras.2014.02.009.

[16] H. Isselé, "Caractérisation et modélisation mécaniques de couches minces pour la fabrication de dispositifs microélectronoiques-application au domaine de l ' intégration 3D," 2014.

[17] P. A. Mante, J. F. Robillard, and A. Devos, "Complete thin film mechanical characterization using picosecond ultrasonics and nanostructured transducers: Experimental demonstration on SiO2," Appl. Phys. Lett., vol. 93, no. 7, pp. 10–13, 2008, doi: 10.1063/1.2975171.

[18] J. E. Pye and C. B. Roth, "Physical aging of polymer films quenched and measured free-standing via ellipsometry: Controlling stress imparted by thermal expansion mismatch between film and support,"

Macromolecules, vol. 46, no. 23, pp. 9455–9463, 2013, doi: 10.1021/ma401872u.

[19] W. A. Brantley, "Calculated elastic constants for stress problems associated with semiconductor devices," J. Appl. Phys., vol. 44, no. 1, pp. 534–535, 1973, doi: 10.1063/1.1661935.

[20] A. Masolin, P.-O. Bouchard, R. Martini, and M. Bernacki, "Thermo-mechanical and fracture properties in single-crystal silicon," J. Mater. Sci., vol. 48, no. 3, pp. 979–988, Feb. 2013, doi: 10.1007/s10853-012-6713-7.

[21] J. S. Blakemore, "Semiconducting and other major properties of gallium arsenide," J. Appl. Phys., vol. 53, no. 10, pp. R123–R181, Oct. 1982, doi: 10.1063/1.331665.

[22] Y. A. Burenkov, Y. M. Burdukov, S. Y. Davidov, and S. P. Nikanorov, "Temperature independences of the elastic constants of gallium arsenide," Sov. Phys. Solid State, vol. 15, no. 6, pp. 1175–1177, 1973.

[23] B. Hajduk, H. Bednarski, and B. Trzebicka, "Temperature-Dependent Spectroscopic Ellipsometry of Thin Polymer Films," J. Phys. Chem. B, vol. 124, no. 16, pp. 3229–3251, Apr. 2020, doi: 10.1021/acs.jpcb.9b11863.

[24] W. Cheng et al., "Elastic properties and glass transition of supported polymer thin films," Macromolecules, vol. 40, no. 20, pp. 7283–7290, 2007, doi: 10.1021/ma071227i.

[25] D. Brick et al., "Glass transition of nanometric polymer films probed by picosecond ultrasonics," Ultrasonics, vol. 119, no. December 2020, p. 106630, 2022, doi: 10.1016/j.ultras.2021.106630.